New insights to the difference in microbial composition and interspecies interactions between fouling layer and mixed liquor in a membrane bioreactor

Revised Manuscript Submitted to

Journal of Membrane Science

Oct 2021

Anh Q. Nguyen[a], Luong N. Nguyen[a], Zhicheng Xu[b], Wenhai Luo[b], Long D. Nghiem[a,*]

[a] Centre for Technology in Water and Wastewater, School of Civil and Environmental Engineering, University of Technology Sydney, Ultimo NSW 2007, Australia

[b] Beijing Key Laboratory of Farmland Soil Pollution Prevention and Remediation, College of Resources and Environmental Sciences, China Agricultural University, Beijing, 100193, China

*Corresponding author:

Long D Nghiem: Centre for Technology in Water and Wastewater, University of Technology Sydney, Ultimo NSW 2007, Australia; E-mail: duclong.nghiem@uts.edu.au

Abstract

This work examined fouling-associated microbial community in a carefully controlled laboratory-scale membrane bioreactor (MBR) at different fouling stages. In agreement with the literature, fouling severity was positively correlated with bound polysaccharide and protein content (indicators) in the mixed liquor. UPGMA clustering analysis with different indices indicated that the biofouling layer (biofilm) and mixed liquor possessed highly similar microbial identity, important differences between the two communities' structures were observed. This is the first comprehensive study to apply differential abundance analysis (ANCOM) to identify microbial taxa driven the divergence in microbial structure including *Victivallales*, *Coxiellales*, unassigned *Microgenomatia* and *Blastocatellia* 11-24 (all presented at <1% abundance). Network analysis also identified *Victivallales* and *Blastocatellia* 11-24 among the few key players in the mixed liquor and biofilm community, respectively. Despite their low abundances, key players in both communities positively correlated (Pearson's correlation coefficient >0.6) with fouling indicators, confirming their important contributions to fouling propensity. The biofilm community exhibited a more complex structure with higher level of inter-species interaction and prevalence of positive connections (74.6%) compared to the mixed liquor community (42.2%), reflecting higher stability and synergy between microbial taxa in the biofilm. Results from this comprehensive investigation can support the development of new fouling control strategies.

Keywords: membrane fouling; microbial community; membrane bioreactors; ecological network; biofilm; mixed liquor.

1. Introduction

Membrane bioreactor process (MBR) has many advantages over the conventional activated sludge process. These include a smaller physical footprint and better effluent quality suitable for water reuse applications [1]. Globally, there are 73 large MBR plants for municipal wastewater with a designed capacity of over 100 ML/d currently in operation or the construction phase (mrbsite.com). There is a much larger number of small and medium MBR plants for municipal and industrial wastewater treatment around the world. Recent scientific progress in membrane fabrication and module design, system integration, and process automation has significantly reduced the cost of wastewater treatment by MBR technology. Thus, there has been a greater focus on membrane fouling which is inherent in any MBR plant and has become a major hurdle for further improvement in energy efficiency and cost-saving [2].

Numerous techniques have been developed and applied to control fouling during MBR operation [2, 3]. They include regular backwashing, membrane cleaning by biocide and oxidising reagents, such as hypochlorite, and modification of membranes and their modules. These techniques are based on chemical and physical processes to remote and disrupt the formation of biofilm on the membrane surface. While they are effective, they cannot completely prevent biofouling regrowth given the direct contact of membrane with microbe-abundant activated sludge (i.e. mixed liquor in MBR). They must be applied frequently, resulting in additional cost and gradual deterioration of membrane performance.

MBR is a biological membrane separation process. As such, biological techniques to control MBR fouling have shown very promising results. Nevertheless, these biological techniques have not yet been applied widely in full-scale operation [4]. In 2009, Lee and co-workers [5] demonstrated for the first time a relationship between microbial quorum sensing activities (i.e. the presence of the N-acyl homoserine lactone quorum signalling molecule) and biofilm formation on the membrane surface. Their work has triggered many subsequent investigations to develop biological techniques to control membrane fouling during MBR operation [6, 7]. Bacteriophage to inhibit specific bacteria in the biofilm is another promising approach to control biofouling [8]. It is essential for these biological techniques to selectively target the biofilm on the membrane surface while maintaining the microbial community in the mixed liquor so that biological performance of the MBR is unaffected. Thus, the key is to understand the difference in microbial composition and inter-species interactions between the biofilm (fouling layer) and mixed liquor.

Recent progress in culture-independent molecular techniques has paved the way for in-depth investigation of the microbial community associated with fouling on the membrane surface in comparison to the mixed liquor [9]. Early works on this topic have focused on characterizing the microbial diversity and composition in the fouling layer and mixed liquor [10-13]; however, inter-

species interactions in each community were rarely examined [14-16]. There is a consensus that the biofilm community differs from the mixed liquor community [13, 14, 17], although the extent of this difference has not been systematically and quantitatively examined. In addition, findings in the literature have been rather inconsistent. For example, Gao et al., [18] reported higher microbial richness and abundance in the bio-cake than that of the bulk sludge. On the other hand, Jo et al. [14] measured biofilm diversity and observed no significant difference from those of activated sludge. Luo et al. [13] reported that the biofilm microbial composition in laboratory-scale MBRs was indistinguishable from that of the mixed liquor during the initial stage of operation but significantly diverged from the sludge over time and ultimately showed a unique biofilm profile. By contrast, Xu et al. [15] observed a greater similarity between the bio-cake and the bulk sludge as the fouling developed.

On a particular note, previous works often assumed that fouling-associated species were highly abundant microbial taxa or taxa that showed higher relative abundance in the biofilm than the mixed liquor [13, 19]. This assumption is problematic because dominant taxa in the biofilm are also abundant in the mixed liquor since the mixed liquor is a major source of inoculum for the biofilm [17]. Thus, their high abundances do not necessarily affirm them as key players in the biofilm community. Through network and biomarker analyses, more recent studies have suggested that low-abundance taxa, rather than high-abundance ones, play critical roles in fouling development and biofilm formation [15, 20-22]. Furthermore, the difference between the biofilm and mixed liquor community based on relative abundance may not reflect the actual difference due to the caveat of relative data. Relative abundances are absolute abundances of different species normalized to the total number of sequences detected in the sample. Thus, the change in the absolute abundance of one microbial species can alter the relative abundance of all other species.

Several bioinformatics tools/analyses have been employed for microbial community characterization in MBRs. Alpha diversity indices describe the number of species in a community (i.e. Chao1 index) and the evenness between their proportions in the community (i.e. Shannon index) [15], while coordination analyses such as principal coordinate analysis (PcoA) and non-metric multidimensional scaling (NMDS) based on beta diversity indices (i.e. unweighted UniFrac and Bray-Curtis) show the similarity/dissimilarity between different communities [17, 23]. Although less popular than coordination analyses, clustering analyses, including the unweighted pair group method with arithmetic mean (UPGMA), can also depict the similarity/dissimilarity between communities and clearly show the pairwise similarities between samples [14, 24, 25]. It is worth noting that the selection of beta diversity index for analysis can influence the extent of dissimilarity between microbial communities since different indices were calculated differently. To address these shortcomings, in recent years, researchers have begun to use network-based techniques for deciphering complex microbial interaction patterns under dynamic conditions such as the composting

of organic waste [26] or to compare the fouling evolution between aerobic and anaerobic MBR [22]. These techniques may also be useful for delineating the difference in microbial composition and inter-species interactions between the fouling layer and mixed liquor in the MBR.

This study addresses key research gaps identified above, such as the lack of attention on the roles of inter-species interactions in fouling, and the impact of the bioinformatics tools and index used for comparison of different microbial communities. This study aims to delineate the distinction between biofouling community (biofilm) and suspended community (mixed liquor) and identify the role of individual microbial taxa in fouling development. Comparison in terms of microbial identity profiles was performed using UPGMA clustering analysis was conducted based on unweighted UniFrac distance metric. Differential abundance analysis (ANCOM) was used to specifically identify species with true different abundance over-represented in each community. Phylogenetic molecular ecological network was constructed for both communities to deduce species-species ecological interactions and the role of high- and low-abundance microbial taxa. Results from this study contribute to a more comprehensive understanding the biofouling microbial community structure to address the problem of membrane fouling in MBR operation.

2. Materials and Methods

2.1. Laboratory-scale membrane bioreactor system setup

A laboratory-scale aerobic membrane bioreactor (MBR) system was used in this study. The MBR was equipped with 6 L glass reactor, a hollow fibre polyvinylidene difluoride membrane module (Mitsubishi Rayon, Japan), a water bath, two peristaltic pumps, a chiller, a pressure sensor and an air pump. The membrane module had a nominal pore size of 0.04 μm and an effective surface area of 0.073 m^2. The pressure sensor was a high-resolution pressure sensor (±0.1 kPa, John Morris Group, Australia), which was installed between the membrane module and the permeate pump for continuous monitoring of the transmembrane pressure (TMP). The chiller (Thermoline Australia) was equipped with a stainless-steel heat-exchanging coil. Two peristaltic pumps (Masterflex L/S, USA) were used for feeding and permeate extraction. The reactor's working volume were maintained at 6.0 L. The air pump (AquaOne, Australia) aerated the reactor at an air flowrate of 400 mL/min via a diffuser at the bottom of the reactor.

2.2. Operating protocol

Activated sludge was transferred from another MBR system (with two identical membrane modules as used in this study). This MBR system was under stable operation for over 2 months and fed with synthetic influent similar to that in this study (Supplementary Information). Synthetic feed was used to provide carbon, nitrogen, and phosphorus for microbial growth in the MBR. The synthetic feed has COD: TN: TP = 150: 6.5: 1, which is similar to the municipal sewage. In details, the synthetic feed

solution (influent) contains mg per litre: glucose (600), peptone (100), urea (35), KH_2PO_4 (17.5), $MgSO_4$ (17.5), $FeSO_4$ (10), and sodium acetate (225) as described in previous studies [27, 28].

During the acclimatisation period, the MBR was operated at different water fluxes in the range from 11 to 15 LMH to determine a suitable value for a reproducible and representative fouling profile. The membrane module was operated with 9 min "suction" and 1 min "relaxation". TMP profiles of these preliminary fouling runs are available in the Supplementary Information. The critical flux was 11 LMH. At flux higher than 11 LMH, the fouling onset was observed within 1-2 days. Based on these preliminary fouling runs, water flux value of 10 LMH used in this study to achieve reproducible and representative fouling under subcritical flux condition. The thresholds for three fouling stages were defined as: no-fouling (TMP $\leq$ 10 kPa) – TMP increases slightly and at slow rate, mild fouling (10 < TMP $\leq$ 30 kPa) – TMP increases exponentially, and severe fouling (TMP > 30 kPa) – TMP increases gradually and tends to reach a plateau.

In the biomass collection period, three repetitive phases were conducted to capture sufficient DNA samples of mixed liquor and biofilm at different fouling stages. The biomass concentration at the beginning of each fouling cycle was set at 12.4 ± 0.1 g/L. When the TMP reached a threshold, the MBR operation was paused and the membrane module was removed from the reactor for DNA sample collection (Section 2.3.2). At the end of each phase, the membrane module was removed for chemical cleaning. The chemical cleaning protocol was able to fully restore to the membrane permeability to as new condition. Sludge withdrawal was conducted to reset the MLSS concentration to around 12. 4 ± 0.1 g/L prior to the next phase.

The performance of the MBR was regularly monitored by sampling effluent, influent, and mixed liquor twice per week. Monitored parameters included pH, dissolved oxygen (DO) concentration in the mixed liquor, effluent turbidity, total organic carbon (TOC), mixed liquor suspended solids (MLSS), mixed liquor volatile suspended solids (MLVSS), extracellular polymeric substance (EPS), soluble microbial products (SMP). MLSS and MLVSS were measured gravimetrically following the method 2540D [29]. TOC was analysed using a TOC-V_{CSH} analyser (Shimadzu, Japan). Nitrate concentration was measured using ion chromatography (Thermo Scientific, Australia). The temperature and DO concentration of the MBR was maintained at 20.0 ± 0.1°C and above 3 mg/L, respectively.

2.3. Analytical methods

2.3.1. Extraction of extracellular polymeric substances and soluble microbial products

EPS and SMP concentrations in mixed liquor samples were measured according to the thermal extraction method [30]. In brief, 25 mL of mixed liquor sample was centrifuged in a 50 mL tube at 1500×g and 4 °C for 20 min to collect SMP fraction. The residual sludge was resuspended with 50 mL of 0.9% NaCl solution at room temperature by a vortex mixer for 3 min. The mixture was transferred

to an enclosed flask and heated at 80 ºC for 1 h to release bound polysaccharide and bound protein (EPS). Then, the mixture was cooled to room temperature before centrifugation at 1500×g and 4 ºC for 20 min. The supernatant was collected for further analysis and denoted as the EPS fraction. The heating method showed high extraction efficiency compared to other physical extraction methods (62 mg EPS/g VSS, yield 4%) [31].

The phenol–sulfuric acid method [32] was applied for determination of polysaccharides with a series of glucose solutions (0.5 – 50 mg/L, calibration curve $R^2 = 0.97$) as the standard. Protein content in EPS and SMP fractions were determined by an UV/VIS spectrophotometer (DR5000, HACH) following the modified Lowry method using Total Protein Kit, Micro Lowry, Peterson′s Modification kit (Sigma-Aldrich) with a series of bovine serum albumin solution as the standard (0.5 – 15 mg/L, calibration curve $R^2 = 0.99$).

2.3.2. DNA extraction and quality monitoring

As mentioned in Section 2.2, duplicate samples of the mixed liquor were collected at the beginning of each phase and at three fouling stages (based on TMP). This resulted in 14 DNA samples. The samples from mixed liquor were labelled as MLx.x.x with ML is mixed liquor; first digit is fouling phase number; second digit is fouling stage; third digit is replication number. For example, ML1.3.1 is the mixed liquor sample at fouling phase 1, fouling stage 3 and replication 1.

Duplicate samples of the membrane biofilm were collected at mild- and severe-fouling stages with minor modifications in each phase. In phase 1, no sample collection was conducted under mild fouling condition in phase 1 to maintain the natural progress of biofilm development. In phase 2, only part of the biofilm was collected from the membrane surface under mild fouling condition to minimalize the impact of sampling on biofilm development. Samples were taken from multiple positions on the membrane surface. In phase 3, the entire biofilm was collected under mild fouling condition thus the phase was terminated and no sample collection was conducted under severe fouling condition. This results in slightly different operational period of each phase: phase 1 (day 14 – 33), phase 2 (day 34 – 49), phase 3 (day 50 – 56). The biofilm (a mixture of cake layer and gel layer deposited on the membrane surface) was scrapped off the membrane surface using cotton swabs prior to membrane chemical cleaning. This resulted in 7 DNA samples. The samples from membrane biofilm were labelled as BFx.x.x with BF: biofilm; first digit is fouling phase number; second digit is fouling stage; third digit is replication number. For example, BF1.3.1 is the biofilm sample at fouling phase 1, fouling stage 3 and replication 1. . Details of samples collection regime in this study is shown in Figure 1 (Section 3.1).

Samples were mixed with ethanol (1:1 v/v) and stored at -20 ºC prior to DNA extraction. Genomic DNA extraction was carried out using QIAamp DNA Stool Mini Kit (Qiagen) following the manual's instructions. An additional bead-beating step was performed at the beginning of the extraction to

enhance DNA yield. The integrity, purity and concentration of the extracted DNA were evaluated by NanoDrop® spectrophotometer. DNA concentration of all samples was normalized to 20 ng/µl using DNase/Pyrogen-Free Water before sending to the sequencing facility.

2.4. Amplicon sequencing and bioinformatics analysis

The universal primer set Pro341F (5'-CCTAYGGGRBGCASCAG-3') and Pro806R (5'-GGACTACNNGGGTATCTAAT-3') was used to amplify 16S rRNA V3 – V4 regions of the microbial community. Paired-end amplicon sequencing (2 × 300 bp) was carried out on the Illumina MiSeq platform (UTS Next Generation Sequencing Facility, Sydney, Australia). Raw sequence data were generated with the Illumina *bcl2fastq* pipeline (version 2.20.0.422). All sequencing data in this study are available at the Sequence Read Archive (accession number: PRJNA752525) in the National Center for Biotechnology Information.

Raw reads were imported into Quantitative Insights into Microbial Ecology (QIIME) 2 (version 2020.11.1) for computational analysis [33]. Quality filtering, denoising (primer and read trimming), paired-end reads merging, dereplication, chimera filtering and feature clustering (≥ 97% similarity) were performed using the q2-dada2 denoise-paired plugin [34]. Forward reads were truncated at position 280 and reverse reads were truncated at position 250 in the 3' end due to decrease in quality. The parameter *min-fold-parent-over-abundance* was set to 4 in the denoising step. Reads were mapped back to amplicon sequence variants (ASV) with a minimum identity of 97% to obtain the number of reads in each feature.

Taxonomy was assigned to features using the q2-feature-classifier [35] classify-sklearn Naïve Bayes taxonomy classifier against the SILVA database (release 132) [36-38] with a confidence of 0.7. All features were aligned with mafft [8] and used to construct phylogenetics tree with FastTree2 [39] via the q2-phylogeny align-to-tree-mafft-fasttree pipeline. Phylogenetic tree was visualized using FigTree (version 1.4.4). Beta diversity metrics (Bray-Curtis dissimilarity) were estimated using q2-diversity core-metrics-phylogenetic pipeline after samples were rarefied (subsampled without replacement) to 25,000 sequences per sample. 2D principal coordinates analysis (PcoA) was plotted using Bray-Curtis distance matrix. Statistical analyses were conducted using QIIME2 to test the difference between the mixed liquor and biofilm communities structure (PERMANOVA test), and identify microbial taxa with differential abundance (analysis of composition of microbiomes - ANCOM) [40]. Results from ANCOM analysis was visualized using RStudio (version 3.6.1).

2.5. Network construction and analysis

The Random Matrix Theory (RMT) based molecular ecological network analysis (MENA) was employed to construct modular networks of microbial taxa in mixed liquor and biofilm at order level [41]. Network analysis can provide insights into microbial co-occurrence patterns in the community, keystone species and interactions between community members, rather than the simple

species richness and abundance. Only taxa detected in at least 4 samples were included in the analysis. Network construction procedures followed the developer's recommendations on the online pipeline, with a correlation cut-off of 0.8 for both mixed liquor and biofilm networks. Networks were constructed based on Pearson's correlation between microbial orders, and the cut-off for network construction was selected based on Chi-square test on Poisson distribution. Networks were modularized using the greedy modularity optimization method. Pearson's correlations between microbial taxa and environmental traits (EPS and SMP concentration) were also determined using MENA pipeline. Network visualization was carried out using Cytoscape (version 3.8.2) [42]. Among-module and within-module connectivity plot was constructed in RStudio (version 3.6.1).

3. Results and Discussion

3.1. Membrane bioreactor performance and fouling development

The MBR system showed stable biological treatment performance and long-term flux profile. High TOC removal (96.3 – 99.1%) was achieved during the experimental period. The average effluent TOC concentration was 3.8 ± 1.6 mg/L. Stable biomass growth was also observed, with biomass concentration (MLSS) increased steadily from around 12 g/L to 18 g/L in 15 days (Supplementary Information). MLVSS/MLSS ratio was above 0.8 throughout the experimental period, indicating high biomass quality.

The TMP profiles of individual fouling phases progressed with the operation times (Figure 1). At the beginning of each fouling phase, TMP gradually increased from 5 to 10 kPa. Once the TMP reached 10 kPa, it increased rapidly to over 30 kPa within 4 days (TMP jump). At TMP higher than 30 kPa, the rate of TMP increase was even higher. Thus, for further analysis, membrane fouling was categorised to three stages: (i) no fouling (TMP <10 kPa), (ii) mild fouling (TMP of 10 to 30 kPa), and severe fouling (TMP >30 kPa). Severe fouling condition was associated with high MLSS content in the reactor (Pearson's correlation $R = 0.79$, p-value < 0.05). The MLSS content was 18 g/L when severe fouling (TMP > 30 kPa) was observed. However, while the increase in MLSS content over time was gradual (Supplementary Information), the increase in TMP was exponential (Figure 1).

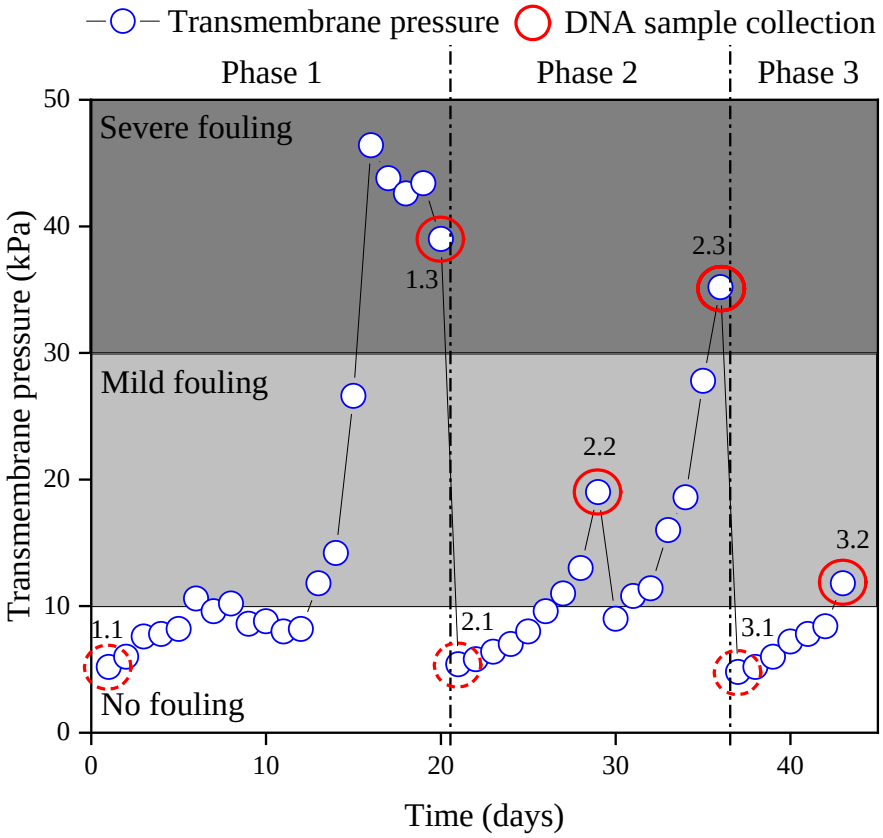

Figure 1. Fouling profile in the membrane bioreactor during the experiment. Each DNA sampling point is marked by a circle and a number. Dashed circles represent the collection of mixed liquor samples only, rounded circles represent the collection of both mixed liquor and biofilm samples. The first digit is the fouling phase number and the second digit is the fouling stage.

There is a correlation between fouling severity and EPS concentration in mixed liquor samples at each fouling phase (Figure 2A&B). EPS and SMP are biopolymers produced by microbial metabolism. Thus, higher microbial activity results in higher release of EPS and SMP. Both EPS and SMP primarily consist of polysaccharides and proteins [43]. The concentration of bound polysaccharides increased proportionally from no fouling to mild fouling and was highest at the severe fouling stage. Similarly, bound protein concentration increased with the three corresponding fouling stages (Figure 2B). This phenomenon can also be observed while normalized bound polysaccharides and proteins to the biomass concentration (Supplementary Information). No clear relationship was observed between fouling and SMP content (i.e. soluble polysaccharides and protein concentration) during the experimental period (Figure 2 C&D).

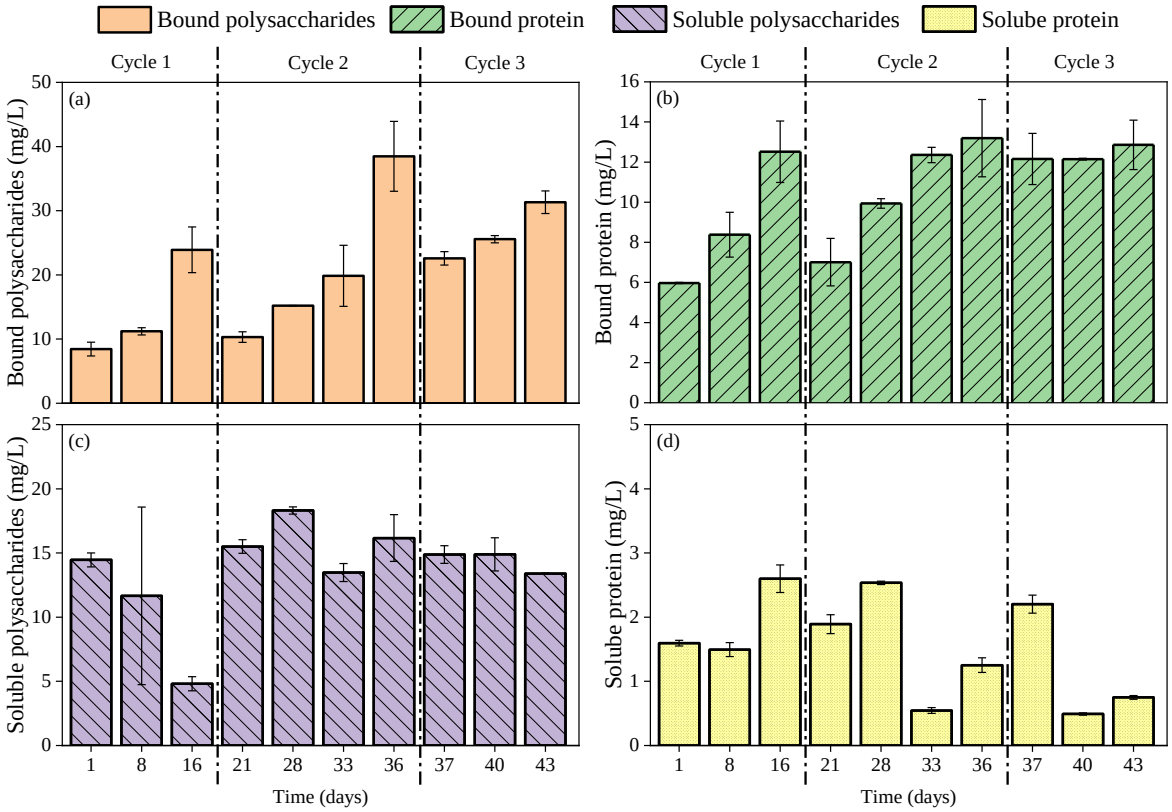

Figure 2. Extracellular polymeric substances (EPS) and soluble microbial products (SMP) concentration in the mixed liquor during the experiment. The error bar represents the standard deviation from duplicate samples.

Results in Figure 2 indicate that EPS governed the fouling process. This is consistent with previous work that reported EPS as a major cause of membrane fouling [25, 44] and correlated strongly with fouling potential and filtration resistance [10, 45]. EPS has been shown to play key role in initial adhesion of microbial biofilm to surfaces [46-48]. In addition, EPS can facilitate cell adhesion [49], cell cohesion and cell communication in biofilm, through dispersion forces, electrostatic interactions, and hydrogen bonds between polymeric substances [46, 50]. This provides the mechanical stability allowing different microorganisms to be retained in long-term close proximity and to establish stable and synergistic community [50]. In addition, both low and excessive production of EPS can weaken the aggregation of microbial sludge flocs in the mixed liquor, and the expanded sludge/small sludge flocs can easily adhered to the surface of the membrane, thereby causing biofouling [44]. The adsorption of EPS on the membrane surface also contribute to organic fouling and can lead to irreversible fouling [51, 52].

A higher concentration of polysaccharide than protein in both EPS and SMP fractions was observed (Figure 2). The protein/polysaccharide (PN/PS) ratio determines specific interactions (e.g. hydrophobic, van der Waals, electrostatic interaction and cation bridging) between sludge flocs and

membrane surface and thus affect membrane fouling [53]. In this study, the PN/PS ratio in EPS and SMP exerted a negative impact on membrane fouling, as fouling propensity increased when PN/PS ratio decreased. The impact of EPS/SMP composition on membrane fouling was also observed in previous studies [53-55]. When protein concentration was constant, flux decline became faster and fouling rate increased as PN/PS ratio decreased for PVDF membrane [55].

3.2. Differences between membrane and mixed liquor microbial communities

3.2.1. Differences in microbial identity

UPGMA clustering analysis was conducted based on unweighted UniFrac distance metric to reconstruct a dendrogram of DNA samples from the MBR (Figure 3). A small but observable dissimilarity in microbial identity profiles can be seen between the mixed liquor and membrane biofilm (Figure 3). Unweighted UniFrac distance metric calculates the distance between pairs of microbial communities based on the presence/absence of observed microorganisms and phylogenetic distances between these microorganisms [56]. The distance between two samples (two tips of the tree) is the sum of all branch lengths connecting between them. Duplicate samples showed small distances to each other (e.g. BF2.3.1 vs BF2.3.2, ML2.1.1 vs. ML2.1.2), confirming the reliability of our sampling procedure and analysis.

The discernible difference between biofilm and mixed liquor samples in terms of microbial identity could be attributed to the presence of unique taxa - specific microbial groups presented in the biofilm that was or was not present (at low abundances) in the mixed liquor and vice versa. This is in agreement with a previous study investigating membrane fouling in five full-scale MBR plants [17]. In this study, the biofilm harvested at the severe fouling stage of phase 1 showed higher similarity to the mixed liquor compared to other biofilms. This is possibly due to the deposition of microbes from the mixed liquor onto the biofilm outer layer due to accumulation of EPS and strong drag force. This observation is also consistent with a previous study by Xu et al., [15] who reported greater similarity between the microbial structure of the biofilm and the mixed liquor as fouling develops at a water flux below the critical flux value.

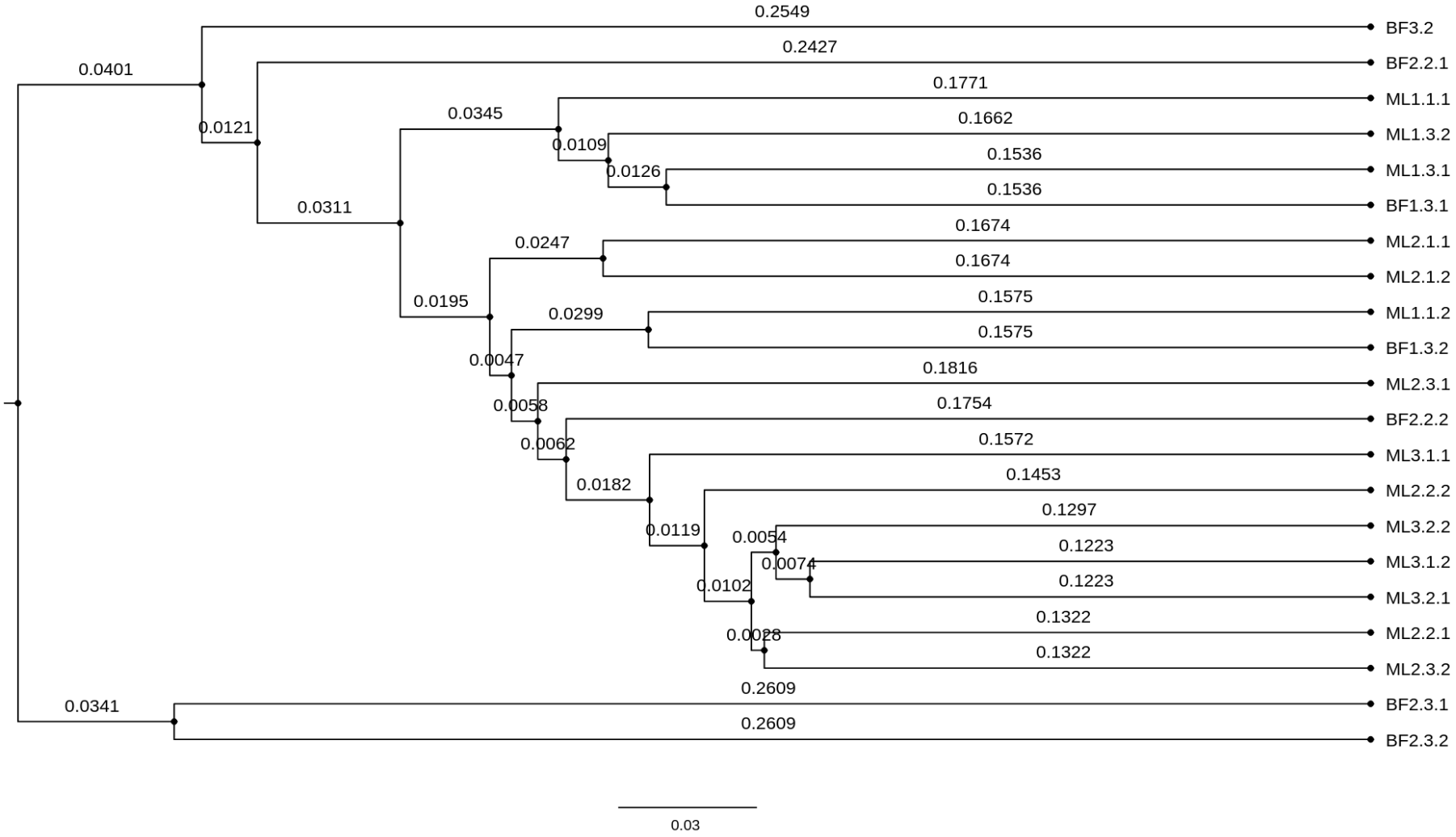

345

346 **Figure 3.** UPGMA clustering dendrogram based on unweighted UniFrac distance metric showing similarity between mixed liquor (ML) and biofilm (BF)
347 microbial identity. BF2.2.2: membrane sample in run 2 fouling stage 2 duplicate 2.

3.2.2. Differences in microbial structure

To highlight the difference in microbial structure between the mixed liquor and biofilm, a dendrogram was constructed by UPGMA clustering analysis using the Bray-Curtis dissimilarity (Figure 4). There is a fundamental difference between the unweighted UniFrac distance metric and Bray-Curtis dissimilarity. While unweighted UniFrac distance metric is a binary (presence/absence) system, Bray-Curtis dissimilarity considers both microbial identity and their abundances. A Bray-Curtis dissimilarity of zero (0) between a pair of samples means these two samples share the same taxa with the same abundance (same structure). As a result, it is expected that the dendrogram based on Bray-Curtis dissimilarity quantifies the difference between the mixed liquor and biofilm in terms of microbial structure. The mixed liquor and biofilm microbial communities become more distinguishable under the microbial structure angle compared to microbial identity angle (Figure 4), indicating that microbial abundance was the key driver of the difference between the two communities. Results from the coordination analysis (PcoA) based on Bray-Curtis dissimilarity also support this finding, with mixed liquor and biofilm samples form distinct clusters (Supplementary Information). The difference between the mixed liquor and biofilm communities was statistically significant (PERMANOVA test, $n = 21$, permutation = 999, pseudo-$F = 3.53$, p-value < 0.05) (Supplementary Information). These results also highlight how diversity index selection strongly impact the extent of difference between the mixed liquor and biofilm communities.

Distinct patterns in microbial structure of biofilm (both early and mature) and mixed liquor have been reported previously in lab [20, 23, 24], pilot [12, 57] and full-scale MBR systems [14, 17]. This difference in microbial structure could be attributed to different assembly mechanisms and environmental conditions [15, 17]. Selective deposition of microorganisms from the mixed liquor to the membrane surface occurs due to multiple factors, such as species mobility and adhesive ability, membrane flux, membrane properties [58]. In addition, biofilm is a microenvironment with high local cell density, resulting in a substantially different level of oxygen and nutrient compared to the mixed liquor [24], with a nutrient concentration gradient forming along the thickness of the biofilm as it developed [59]. As such, microorganisms that can adapt to these conditions emerge in the biofilm community, and further drive the divergence between biofilm and mixed liquor microbial structure.

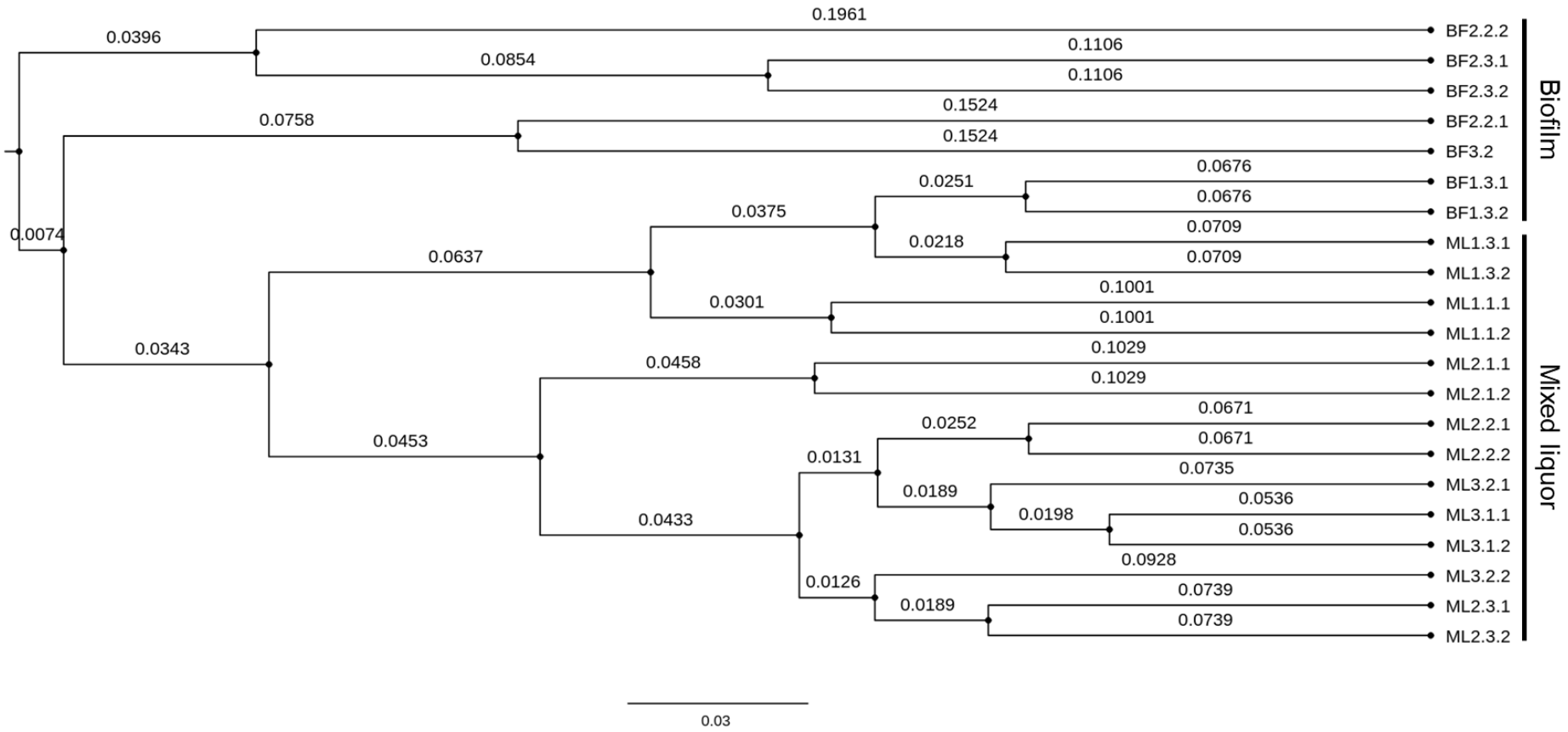

Figure 4. UPGMA clustering based on unweighted Bray-Curtis dissimilarity showing difference between mixed liquor (ML) and biofilm (BF) microbial structure. BF2.2.2: membrane sample in run 2 fouling stage 2 duplicate 2.

3.2.3. Difference in microbial abundance

Since the difference between the two communities was mainly caused by difference in microbial abundance (Section 3.2.2), microbial abundance was further examined. Differential abundance analysis was performed to identify specific microbial taxa that steers the divergence between mixed liquor and biofilm communities. Differential abundance analysis can be used to identify taxa that present in different absolute abundances across two or more environments (sample groups) [60]. In this study, a log-ratio based normalization method (known as ANCOM) was used for differential abundance analysis. This method successively uses each taxon as the reference taxon and transforms the observed abundances to log ratios of the observed abundance each taxon relative to the reference taxon [40]. It controls the false discovery rate at the low level (5%) while maintaining high statistical power [60].

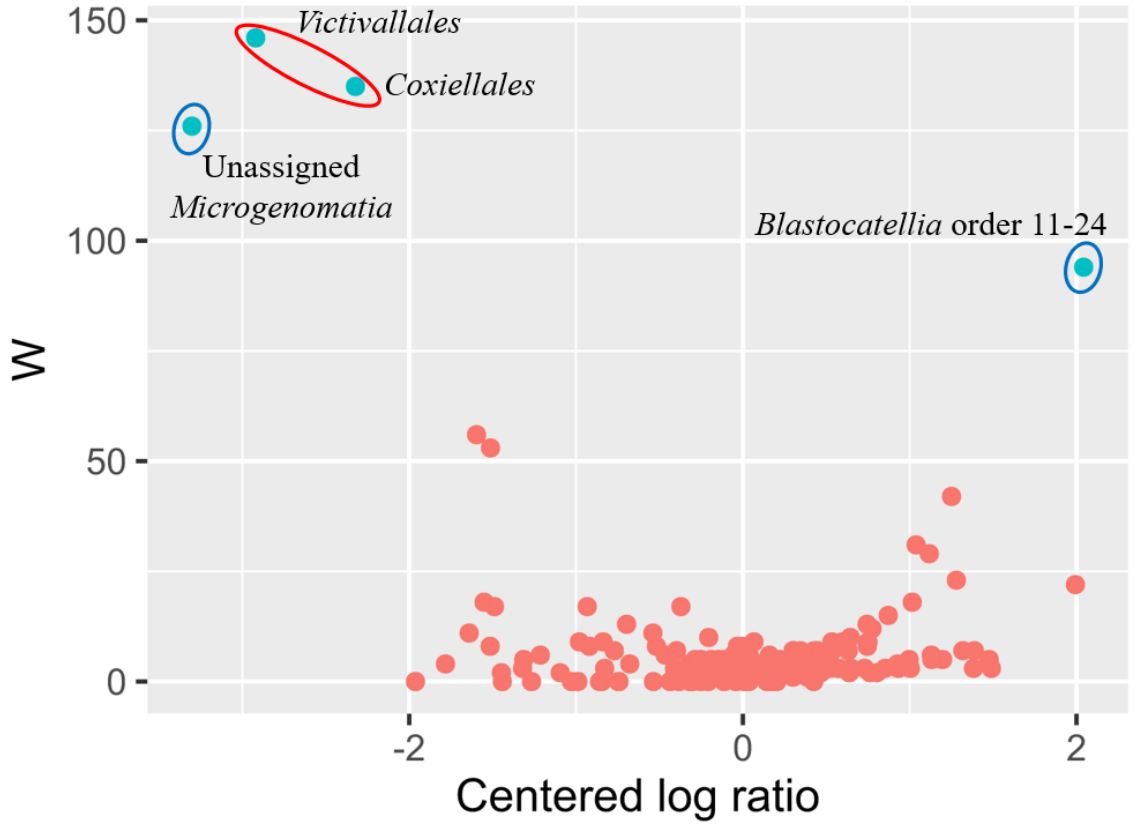

Figure 5. Differential abundance analysis (ANCOM) volcano plot. The W value represents the number of times the null-hypothesis (the average abundance of a given order in the mixed liquor is equal to that in the biofilm) was rejected for a given order. When the W value of an order is high, it is more likely that the order is differentially abundant across sample groups. The 70th percentile of the W distribution is used as the empirical cut-off value. Orders with W values higher than this cut-off is labelled with red circles, and orders with high W values but less than the cut-off is labelled with blue circles. The centered log ratio (clr) is the transformed mean difference in abundance of a given order

between the mixed liquor and biofilm groups. A positive clr means an order is abundant in mixed lqiuor and a negative clr value means a species is abundant in biofilm.

Figure 5 shows only a few orders of differential abundance between mixed liquor and biofilm samples. The W value for an order means that the ratio between that order and W other orders was different across the compared sample groups. Higher W value means higher likelihood that the difference is true [60]. Compared to mixed liquor samples, *Victivallales*, *Coxiellales* and unassigned *Microgenomatia* were enriched in biofilm samples, while *Blastocatellia* order 11-24 was depleted in biofilm samples. Despite their preferential growth in the biofilm, together *Victivallales*, *Coxiellales* and unassigned *Microgenomatia* only account for a small fraction (<1%) of the biofilm microbial community and can be defined as rare taxa. Rare taxa (<1%) have been identified as biomarker shaping the difference between MBR bulk sludge and biofilm communities [17], and it was also suggested that these rare taxa play important roles in fouling development [20]. Results in Figure 5 corroborate with observation from microbial identity analysis (section 3.2.1) to confirm the difference in microbial community structure between the mixed liquor and the biofilm on the membrane surface.

3.2.4. Key players in mixed liquor compared to biofilm community

Modularized RMT-based ecological networks of mixed liquor and biofilm microbial communities were constructed to reveal the microbial interactions within each community (Figure 6 & Table 1). Cooperative and competing interactions can exist between microbial taxa in a community. Examples of cooperative interactions are cross-feeding, where a taxa feeds on the microbial product of another taxa [61], or mutualistic symbiosis where both taxa benefit from the relationship [62]. Microbial taxa can also compete with each other for carbon sources and other nutrients (e.g. oxygen, nitrogen) due to limited space and nutritional resources. The average clustering coefficient, path distance, and modularity of the two empirical networks were significantly higher than that of their corresponding random networks under identical nodes and links, indicating its small-world behaviour and modularity structure (Table 1). The nodes in the network mainly affiliated to the phylum *Proteobacteria*, *Patescibacteria*, *Acidobacteria*, and *Bacteroidetes* (Figure 6), which have been identified as dominant wastewater phyla.

425 **Table 1.** Major topological properties of empirical and random molecular ecological networks (MENs) of bacterial community in mixed liquor and biofilm.

Sample type	Empirical network						100 random networks		
	Total nodes	Total edges	Average degree	Average clustering coefficient	Average path distance	Modularity	Average clustering coefficient	Average path distance	Modularity
Mixed liquor	66	90	2.727	0.186	4.279	0.622	0.04 ± 0.02	3.65 ± 0.16	0.55 ± 0.02
Biofilm	99	354	7.152	0.363	3.423	0.499	0.12 ± 0.01	2.6 ± 0.03	0.29 ± 0.01

426

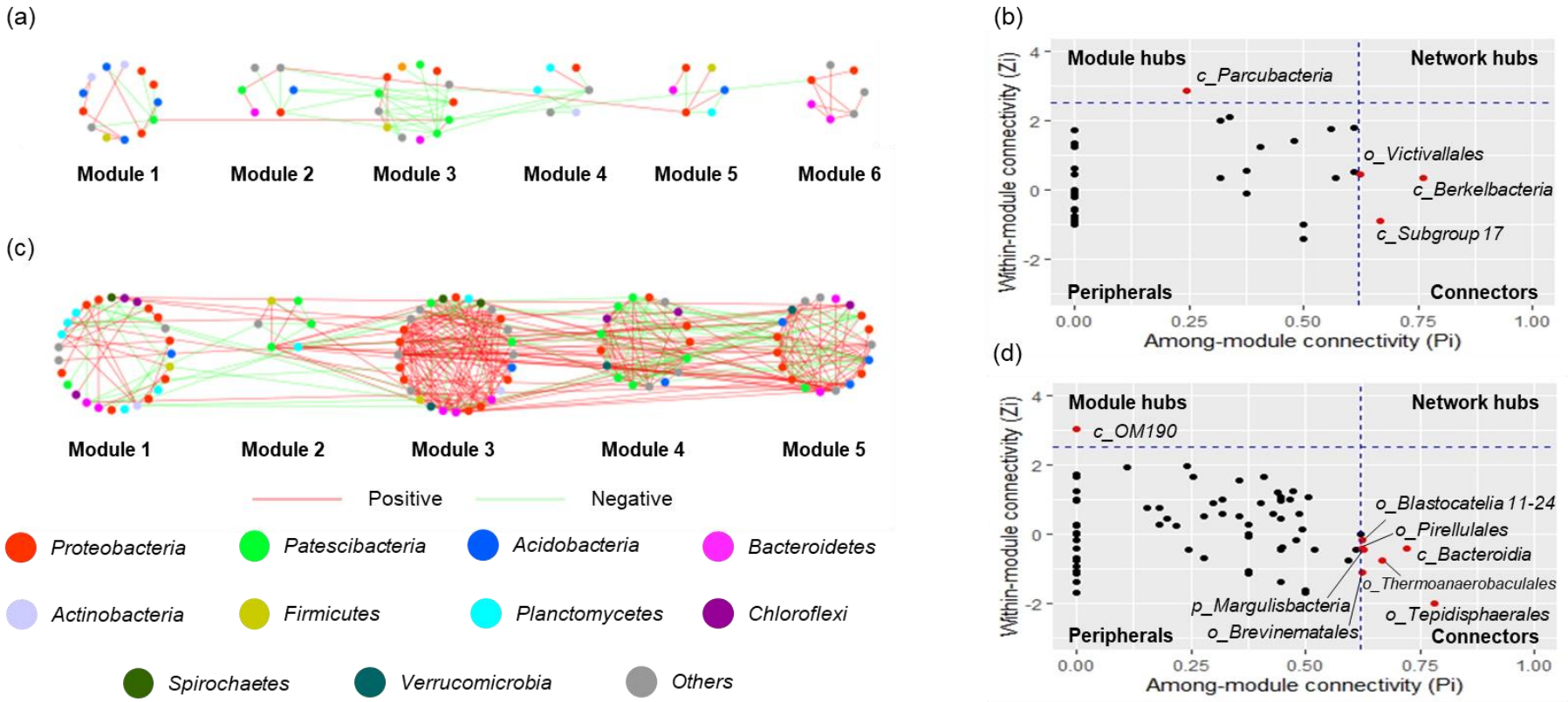

Figure 6. Modularized co-occurrence network analysis revealing the interactions among microbial orders in (a) the mixed liquor and (c) the biofilm community with Z-P plot of species topological roles (b&d). The formed modules with the number nodes more than 5 were selected to construct final modularized co-occurrence network. Each node represents a microbial order. The nodes' colors represent different major phyla (account for >75% of network members). Red and green lines represent positive and negative interactions, respectively.

A higher level of interaction between microbial orders was observed in the biofilm compared to the mixed liquor, indicated by the higher number of nodes, edges, average degree (connectivity) and clustering coefficient (Table 1), suggesting the existence of a more complex microbial structure in the biofilm [15]. The higher connectivity also reflects higher stability of the microbial community in the biofilm compared to the mixed liquor, since the removal of a small number of edges will not be able weaken the network. In addition, more positive connections were observed in the biofilm (74.6%) compared to the mixed liquor (42.2%) (Figure 6), suggesting the predominance of syntrophic and mutual relationships in the biofilm. This agrees with assembly mechanisms of mixed liquor and biofilm. Microbial taxa in the mixed liquor are more dispersed [63], while those in the biofilm are placed in close proximity, allowing for intense communication and high synergy, and resulting in their stable co-existence [50].

Microbial orders in each module were densely connected among one another (especially in the biofilm network) and each module could be regarded as a functional ecological unit. The topological role of a taxa could be defined by its position compared with others in its own module and how well it connects to taxa in other modules. As shown in the Z-P plot (Figure 6B&D), the majority of nodes were detected as peripherals with most of their links inside their own modules (93.9 and 91.9% in the mixed liquor and biofilm network, respectively). Only 3 nodes (4.6%) in the mixed liquor network and 6 nodes (7.1%) in the biofilm network were identified as connectors that are highly connected to several modules and are likely to be key players in the community.

A common characteristic between the biofilm and mixed liquor networks is all identified connectors was orders with low relative abundances. For example, the two connectors *Victivallales* and uncultured *Berkelbacteria* only accounted for <0.3% in the mixed liquor community. Similarly, many connectors have negligible to low relative abundance in the biofilm, e.g. *Pirellulales*, *Tepidisphaerales* and unassigned *Bacteroidia* <0.2%. Xu et al. [15] and Zhang et al. [20] also observed that keystone fouling-causing taxa in biofilm networks were present at very low abundances (0.01%–0.93%). By contrast, dominant orders such as *Betaproteobacteriales* and *Chitinophagales* did not appear to play important roles in both communities. These two dominant orders accounted for 55.4 ± 6.1% of the mixed liquor community and 41.8 ± 10.0% of the biofilm community, respectively).

The relationships between microbial taxa with environmental traits were established by the Pearson correlation (Supplementary Information). The majority of network connectors strongly correlated (correlation coefficient > 0.6) with EPS and SMP, further confirming their contributions to fouling. A higher number of correlation was observed between microbial taxa in the biofilm and fouling indicators than that of the mixed liquor. These results suggest that the biofilm microbial community is more fouling-associated. In addition, since keystone fouling-causing taxa only occur in the fouling layer at a very low abundance (<1%), it may be possible to independently regulate them to control fouling without affecting biological performance of the mixed liquor. For example, bacteriophage – a virus that infects and destroy specific host bacterium through cell lysis/disruption actions – can be used to eliminate these fouling-associated taxa in the community [64, 65], with minimal unintentional ecological impacts on other taxa [66]. Goldman et al. [67] demonstrated that phages targeting *Pseudomonas aeruginosa*, *Acinetobacter johnsonii* and *Bacillus subtilis* can reduce membrane biofouling by 40% to >60% in ultrafiltration system. Ma et al. [68] also reported effective fouling mitigation with different bacteriophage assisted anti-biofouling strategies in ultrafiltration including phage immobilization on the membrane surface in dead-end filtration system, phage addition into the feed of cross-flow, and phage-assisted cleaning of a biofouled membrane.

4. Conclusion

This study highlights the importance of bioinformatics analysis and index selection for microbial community characterization. Using a combination of complementary bioinformatics analyses (i.e. UPGMA clustering analysis, differential abundance analysis and network analysis), this study provides a more complete picture of the difference in microbial community between the fouling layer (biofilm) and mixed liquor and helps to reconcile the discrepancy in the current literature. There is a subtle but critical difference in microbial community structure between the fouling layer and mixed liquor. Although broadly similar in the composition of abundant microbial taxa, the fouling layer (biofilm) shows a higher level of inter-species interaction. Key drivers of the critical difference between the fouling layer and mixed liquor were identified to be low-abundance taxa (<1%) which formed multiple syntrophic interactions with more abundant taxa in the community. These keystone fouling-causing taxa in the fouling layer appear to play critical role in communication and forming syntrophic and mutual interaction with other more abundant taxa within the network. Results from this study are useful for the development of biological techniques that target these specific low-abundance fouling-associated taxa to control fouling in MBR applications.

5. Acknowledgement

The authors acknowledge financial support from the Australia Research Council, Australia through the ARC Research Hub for Energy-efficient Separation (IH170100009). Anh Q. Nguyen gratefully acknowledges a Research Training Scholarship from the University of Technology Sydney.

REFERENCES

[1] L.D. Nghiem, L.N. Nguyen, H.V. Phan, H.H. Ngo, W. Guo, F. Hai, 7 - Aerobic membrane bioreactors and micropollutant removal, in: H.Y. Ng, T.C.A. Ng, H.H. Ngo, G. Mannina, A. Pandey (Eds.) Current Developments in Biotechnology and Bioengineering, Elsevier, 2020, pp. 147-162.

[2] P. Krzeminski, L. Leverette, S. Malamis, E. Katsou, Membrane bioreactors – A review on recent developments in energy reduction, fouling control, novel configurations, LCA and market prospects, Journal of Membrane Science, 527 (2017) 207-227.

[3] X.C. Xiaolei Zhang, Jiayao Reng, Xiao Ma, Qiang Liu, Ping Yao, Hao H. Ngo, and Long D. Nghiem, UV assisted backwashing for fouling control in membrane bioreactor operation, Journal of Membrane Science, 639 (2021) 119751.

[4] Z. Wang, J. Ma, C.Y. Tang, K. Kimura, Q. Wang, X. Han, Membrane cleaning in membrane bioreactors: A review, Journal of Membrane Science, 468 (2014) 276-307.

[5] K.-M. Yeon, W.-S. Cheong, H.-S. Oh, W.-N. Lee, B.-K. Hwang, C.-H. Lee, H. Beyenal, Z. Lewandowski, Quorum Sensing: A New Biofouling Control Paradigm in a Membrane Bioreactor for Advanced Wastewater Treatment, Environmental Science & Technology, 43 (2009) 380-385.

[6] H.-S. Oh, C.-H. Lee, Origin and evolution of quorum quenching technology for biofouling control in MBRs for wastewater treatment, Journal of Membrane Science, 554 (2018) 331-345.

[7] H.-W. Kim, H.-S. Oh, S.-R. Kim, K.-B. Lee, K.-M. Yeon, C.-H. Lee, S. Kim, J.-K. Lee, Microbial population dynamics and proteomics in membrane bioreactors with enzymatic quorum quenching, Applied Microbiology and Biotechnology, 97 (2013) 4665-4675.

[8] Y. Cui, H. Gao, R. Yu, L. Gao, M. Zhan, Biological-based control strategies for MBR membrane biofouling: a review, Water Science and Technology, 83 (2021) 2597-2614.

[9] L.N. Nguyen, A.S. Commault, T. Kahlke, P.J. Ralph, G.U. Semblante, M.A.H. Johir, L.D. Nghiem, Genome sequencing as a new window into the microbial community of membrane bioreactors – A critical review, Science of The Total Environment, 704 (2020) 135279.

[10] D.-W. Gao, Z.-D. Wen, B. Li, H. Liang, Membrane fouling related to microbial community and extracellular polymeric substances at different temperatures, Bioresource Technology, 143 (2013) 172-177.

[11] Y. Miura, Y. Watanabe, S. Okabe, Membrane Biofouling in Pilot-Scale Membrane Bioreactors (MBRs) Treating Municipal Wastewater: Impact of Biofilm Formation, Environmental Science & Technology, 41 (2007) 632-638.

[12] A. Piasecka, C. Souffreau, K. Vandepitte, L. Vanysacker, R.M. Bilad, T. De Bie, B. Hellemans, L. De Meester, X. Yan, P. Declerck, I.F.J. Vankelecom, Analysis of the microbial community structure in a membrane bioreactor during initial stages of filtration, Biofouling, 28 (2012) 225-238.

[13] J. Luo, P. Lv, J. Zhang, A.G. Fane, D. McDougald, S.A. Rice, Succession of biofilm communities responsible for biofouling of membrane bio-reactors (MBRs), PloS one, 12 (2017) e0179855-e0179855.

[14] S.J. Jo, H. Kwon, S.-Y. Jeong, C.-H. Lee, T.G. Kim, Comparison of microbial communities of activated sludge and membrane biofilm in 10 full-scale membrane bioreactors, Water Research, 101 (2016) 214-225.
[15] R. Xu, Z. Yu, S. Zhang, F. Meng, Bacterial assembly in the bio-cake of membrane bioreactors: Stochastic vs. deterministic processes, Water Research, 157 (2019) 535-545.
[16] S.-Y. Jeong, T. Yi, C.-H. Lee, T.G. Kim, Spatiotemporal dynamics and correlation networks of bacterial and fungal communities in a membrane bioreactor, Water Research, 105 (2016) 218-230.
[17] G.K. Matar, S. Bagchi, K. Zhang, D.B. Oerther, P.E. Saikaly, Membrane biofilm communities in full-scale membrane bioreactors are not randomly assembled and consist of a core microbiome, Water Research, 123 (2017) 124-133.
[18] D.-W. Gao, Z.-D. Wen, B. Li, H. Liang, Microbial community structure characteristics associated membrane fouling in A/O-MBR system, Bioresource Technology, 154 (2014) 87-93.
[19] T. Inaba, T. Hori, H. Aizawa, A. Ogata, H. Habe, Architecture, component, and microbiome of biofilm involved in the fouling of membrane bioreactors, NPJ biofilms and microbiomes, 3 (2017) 5-5.
[20] S. Zhang, Z. Zhou, Y. Li, F. Meng, Deciphering the core fouling-causing microbiota in a membrane bioreactor: Low abundance but important roles, Chemosphere, 195 (2018) 108-118.
[21] S. Ishizaki, T. Fukushima, S. Ishii, S. Okabe, Membrane fouling potentials and cellular properties of bacteria isolated from fouled membranes in a MBR treating municipal wastewater, Water Research, 100 (2016) 448-457.
[22] Y. Yao, R. Xu, Z. Zhou, F. Meng, Linking dynamics in morphology, components, and microbial communities of biocakes to fouling evolution: A comparative study of anaerobic and aerobic membrane bioreactors, Chemical Engineering Journal, 413 (2021) 127483.
[23] Y. Takimoto, M. Hatamoto, T. Ishida, T. Watari, T. Yamaguchi, Fouling Development in A/O-MBR under Low Organic Loading Condition and Identification of Key Bacteria for Biofilm Formations, Scientific Reports, 8 (2018) 11427.
[24] P.-N. Hong, M. Noguchi, N. Matsuura, R. Honda, Mechanism of biofouling enhancement in a membrane bioreactor under constant trans-membrane pressure operation, Journal of Membrane Science, 592 (2019) 117391.
[25] D.-w. Gao, Y. Fu, Y. Tao, X.-x. Li, M. Xing, X.-h. Gao, N.-q. Ren, Linking microbial community structure to membrane biofouling associated with varying dissolved oxygen concentrations, Bioresource Technology, 102 (2011) 5626-5633.
[26] Z. Xu, C. Qi, L. Zhang, Y. Ma, G. Li, L.D. Nghiem, W. Luo, Regulating bacterial dynamics by lime addition to enhance kitchen waste composting, Bioresource Technology, (2021) 125749.
[27] L.N. Nguyen, F.I. Hai, J. Kang, W.E. Price, L.D. Nghiem, Removal of emerging trace organic contaminants by MBR-based hybrid treatment processes, International Biodeterioration & Biodegradation, 85 (2013) 474-482.

[28] K.C. Wijekoon, F.I. Hai, J. Kang, W.E. Price, W. Guo, H.H. Ngo, T.Y. Cath, L.D. Nghiem, A novel membrane distillation–thermophilic bioreactor system: Biological stability and trace organic compound removal, Bioresource Technology, 159 (2014) 334-341.
[29] L.C. AD Eaton, EW Rice, AE Greenberg, Standard Methods for the Examination of Water and Wastewater, 21 ed., APHA, Washington DC, New York, 2005.
[30] J.A.P. R.S. Hanson, Chemical composition, in: P. Gerhardt (Ed.) Manual of methods for general bacteriology, American Society for Microbiology, Washington, D.C, 1981, pp. 328–364.
[31] S. Comte, G. Guibaud, M. Baudu, Relations between extraction protocols for activated sludge extracellular polymeric substances (EPS) and EPS complexation properties: Part I. Comparison of the efficiency of eight EPS extraction methods, Enzyme and Microbial Technology, 38 (2006) 237-245.
[32] M. Dubois, K. Gilles, J.K. Hamilton, P.A. Rebers, F. Smith, A Colorimetric Method for the Determination of Sugars, Nature, 168 (1951) 167-167.
[33] E. Bolyen, J.R. Rideout, M.R. Dillon, N.A. Bokulich, C.C. Abnet, G.A. Al-Ghalith, H. Alexander, E.J. Alm, M. Arumugam, F. Asnicar, Y. Bai, J.E. Bisanz, K. Bittinger, A. Brejnrod, C.J. Brislawn, C.T. Brown, B.J. Callahan, A.M. Caraballo-Rodríguez, J. Chase, E.K. Cope, R. Da Silva, C. Diener, P.C. Dorrestein, G.M. Douglas, D.M. Durall, C. Duvallet, C.F. Edwardson, M. Ernst, M. Estaki, J. Fouquier, J.M. Gauglitz, S.M. Gibbons, D.L. Gibson, A. Gonzalez, K. Gorlick, J. Guo, B. Hillmann, S. Holmes, H. Holste, C. Huttenhower, G.A. Huttley, S. Janssen, A.K. Jarmusch, L. Jiang, B.D. Kaehler, K.B. Kang, C.R. Keefe, P. Keim, S.T. Kelley, D. Knights, I. Koester, T. Kosciolek, J. Kreps, M.G.I. Langille, J. Lee, R. Ley, Y.-X. Liu, E. Loftfield, C. Lozupone, M. Maher, C. Marotz, B.D. Martin, D. McDonald, L.J. McIver, A.V. Melnik, J.L. Metcalf, S.C. Morgan, J.T. Morton, A.T. Naimey, J.A. Navas-Molina, L.F. Nothias, S.B. Orchanian, T. Pearson, S.L. Peoples, D. Petras, M.L. Preuss, E. Pruesse, L.B. Rasmussen, A. Rivers, M.S. Robeson, P. Rosenthal, N. Segata, M. Shaffer, A. Shiffer, R. Sinha, S.J. Song, J.R. Spear, A.D. Swafford, L.R. Thompson, P.J. Torres, P. Trinh, A. Tripathi, P.J. Turnbaugh, S. Ul-Hasan, J.J.J. van der Hooft, F. Vargas, Y. Vázquez-Baeza, E. Vogtmann, M. von Hippel, W. Walters, Y. Wan, M. Wang, J. Warren, K.C. Weber, C.H.D. Williamson, A.D. Willis, Z.Z. Xu, J.R. Zaneveld, Y. Zhang, Q. Zhu, R. Knight, J.G. Caporaso, Reproducible, interactive, scalable and extensible microbiome data science using QIIME 2, Nature Biotechnology, 37 (2019) 852-857.
[34] B.J. Callahan, P.J. McMurdie, M.J. Rosen, A.W. Han, A.J.A. Johnson, S.P. Holmes, DADA2: High-resolution sample inference from Illumina amplicon data, Nature Methods, 13 (2016) 581-583.
[35] N.A. Bokulich, B.D. Kaehler, J.R. Rideout, M. Dillon, E. Bolyen, R. Knight, G.A. Huttley, J. Gregory Caporaso, Optimizing taxonomic classification of marker-gene amplicon sequences with QIIME 2's q2-feature-classifier plugin, Microbiome, 6 (2018) 90.
[36] F.O. Glöckner, P. Yilmaz, C. Quast, J. Gerken, A. Beccati, A. Ciuprina, G. Bruns, P. Yarza, J. Peplies, R. Westram, W. Ludwig, 25 years of serving the community with ribosomal RNA gene reference databases and tools, Journal of Biotechnology, 261 (2017) 169-176.

[37] P. Yilmaz, L.W. Parfrey, P. Yarza, J. Gerken, E. Pruesse, C. Quast, T. Schweer, J. Peplies, W. Ludwig, F.O. Glöckner, The SILVA and "All-species Living Tree Project (LTP)" taxonomic frameworks, Nucleic Acids Res, 42 (2013) D643-D648.
[38] C. Quast, E. Pruesse, P. Yilmaz, J. Gerken, T. Schweer, P. Yarza, J. Peplies, F.O. Glöckner, The SILVA ribosomal RNA gene database project: improved data processing and web-based tools, Nucleic Acids Res, 41 (2012) D590-D596.
[39] M.N. Price, P.S. Dehal, A.P. Arkin, FastTree 2 – Approximately Maximum-Likelihood Trees for Large Alignments, PLOS ONE, 5 (2010) e9490.
[40] S. Mandal, W. Van Treuren, R.A. White, M. Eggesbø, R. Knight, S.D. Peddada, Analysis of composition of microbiomes: a novel method for studying microbial composition, Microb Ecol Health Dis, 26 (2015) 27663-27663.
[41] Y. Deng, Y.-H. Jiang, Y. Yang, Z. He, F. Luo, J. Zhou, Molecular ecological network analyses, BMC Bioinformatics, 13 (2012) 113.
[42] P. Shannon, A. Markiel, O. Ozier, N.S. Baliga, J.T. Wang, D. Ramage, N. Amin, B. Schwikowski, T. Ideker, Cytoscape: a software environment for integrated models of biomolecular interaction networks, Genome Res, 13 (2003) 2498-2504.
[43] P. Di Martino, Extracellular polymeric substances, a key element in understanding biofilm phenotype, AIMS Microbiol, 4 (2018) 274-288.
[44] X. Du, Y. Shi, V. Jegatheesan, I.U. Haq, A Review on the Mechanism, Impacts and Control Methods of Membrane Fouling in MBR System, Membranes, 10 (2020) 24.
[45] R. Maddela Naga, Z. Zhou, Z. Yu, S. Zhao, F. Meng, S.-J. Liu, Functional Determinants of Extracellular Polymeric Substances in Membrane Biofouling: Experimental Evidence from Pure-Cultured Sludge Bacteria, Applied and Environmental Microbiology, 84 (2018) e00756-00718.
[46] O.Y.A. Costa, J.M. Raaijmakers, E.E. Kuramae, Microbial Extracellular Polymeric Substances: Ecological Function and Impact on Soil Aggregation, Frontiers in Microbiology, 9 (2018).
[47] P. Entcheva-Dimitrov, M. Spormann Alfred, Dynamics and Control of Biofilms of the Oligotrophic Bacterium Caulobacter crescentus, Journal of Bacteriology, 186 (2004) 8254-8266.
[48] Z. Wan, P.J.B. Brown, E.N. Elliott, Y.V. Brun, The adhesive and cohesive properties of a bacterial polysaccharide adhesin are modulated by a deacetylase, Molecular Microbiology, 88 (2013) 486-500.
[49] Y. Zhu, Y. Zhang, H.-q. Ren, J.-j. Geng, K. Xu, H. Huang, L.-l. Ding, Physicochemical characteristics and microbial community evolution of biofilms during the start-up period in a moving bed biofilm reactor, Bioresource Technology, 180 (2015) 345-351.
[50] H.-C. Flemming, J. Wingender, The biofilm matrix, Nat Rev Microbiol, 8 (2010) 623-633.
[51] O.T. Iorhemen, R.A. Hamza, J.H. Tay, Membrane Bioreactor (MBR) Technology for Wastewater Treatment and Reclamation: Membrane Fouling, Membranes, 6 (2016) 33.

643 [52] A. Ramesh, D.J. Lee, J.Y. Lai, Membrane biofouling by extracellular polymeric substances or
644 soluble microbial products from membrane bioreactor sludge, Applied Microbiology and
645 Biotechnology, 74 (2007) 699-707.
646 [53] L. Hao, S.N. Liss, B.Q. Liao, Influence of COD:N ratio on sludge properties and their role in
647 membrane fouling of a submerged membrane bioreactor, Water Research, 89 (2016) 132-141.
648 [54] T.C.A. Ng, H.Y. Ng, Characterisation of initial fouling in aerobic submerged membrane
649 bioreactors in relation to physico-chemical characteristics under different flux conditions, Water
650 Research, 44 (2010) 2336-2348.
651 [55] M. Yao, K. Zhang, L. Cui, Characterization of protein–polysaccharide ratios on membrane
652 fouling, Desalination, 259 (2010) 11-16.
653 [56] C. Lozupone, R. Knight, UniFrac: a new phylogenetic method for comparing microbial
654 communities, Applied and Environmental Microbiology, 71 (2005) 8228-8235.
655 [57] S. Lim, S. Kim, K.-M. Yeon, B.-I. Sang, J. Chun, C.-H. Lee, Correlation between microbial
656 community structure and biofouling in a laboratory scale membrane bioreactor with synthetic
657 wastewater, Desalination, 287 (2012) 209-215.
658 [58] F. Meng, B. Liao, S. Liang, F. Yang, H. Zhang, L. Song, Morphological visualization,
659 componential characterization and microbiological identification of membrane fouling in membrane
660 bioreactors (MBRs), Journal of Membrane Science, 361 (2010) 1-14.
661 [59] W.J. Gao, H.J. Lin, K.T. Leung, H. Schraft, B.Q. Liao, Structure of cake layer in a submerged
662 anaerobic membrane bioreactor, Journal of Membrane Science, 374 (2011) 110-120.
663 [60] H. Lin, S.D. Peddada, Analysis of microbial compositions: a review of normalization and
664 differential abundance analysis, npj Biofilms and Microbiomes, 6 (2020) 60.
665 [61] H. Celiker, J. Gore, Cellular cooperation: insights from microbes, Trends in Cell Biology, 23
666 (2013) 9-15.
667 [62] F. Ju, T. Zhang, Bacterial assembly and temporal dynamics in activated sludge of a full-scale
668 municipal wastewater treatment plant, The ISME Journal, 9 (2015) 683-695.
669 [63] H. Aqeel, D.G. Weissbrodt, M. Cerruti, G.M. Wolfaardt, B.-M. Wilén, S.N. Liss, Drivers of
670 bioaggregation from flocs to biofilms and granular sludge, Environmental Science: Water Research &
671 Technology, 5 (2019) 2072-2089.
672 [64] S. Ayyaru, J. Choi, Y.-H. Ahn, Biofouling reduction in a MBR by the application of a lytic phage
673 on a modified nanocomposite membrane, Environ. Sci.: Water Res. Technol., 4 (2018) 1624-1638.
674 [65] G. Scarascia, S.A. Yap, A.H. Kaksonen, P.-Y. Hong, Bacteriophage Infectivity Against
675 Pseudomonas aeruginosa in Saline Conditions, Frontiers in Microbiology, 9 (2018) 875.
676 [66] G. Scarascia, S.A. Yap, A.H. Kaksonen, P.-Y. Hong, Bacteriophage Infectivity Against
677 Pseudomonas aeruginosa in Saline Conditions, Frontiers in Microbiology, 9 (2018).
678 [67] G. Goldman, J. Starosvetsky, R. Armon, Inhibition of biofilm formation on UF membrane by use
679 of specific bacteriophages, Journal of Membrane Science, 342 (2009) 145-152.

[68] W. Ma, M. Panecka, N. Tufenkji, M.S. Rahaman, Bacteriophage-based strategies for biofouling control in ultrafiltration: In situ biofouling mitigation, biocidal additives and biofilm cleanser, Journal of Colloid and Interface Science, 523 (2018) 254-265.